INTRODUCTION

Colorectal cancer is the third leading cause of cancer deaths worldwide. The number of patients affected by this disease continues to increase steadily (1–3) and ~42 000 deaths occur annually in Japan (3).

FOLFOX4, a bi-weekly schedule of intravenous bolus and infusional 5-fluorouracil/folinic acid plus oxaliplatin (Elplat®) is a widely used regimen for the first-line treatment of metastatic colorectal cancer (MCRC) (4,5). However, oral fluoropyrimidines can replace the intravenous fluoropyrimidine component of combination regimens. Capecitabine (Xeloda®) is an oral fluoropyrimidine with similar efficacy to bolus 5-fluorouracil/folinic acid when given as first-line treatment for MCRC (6–8) or as adjuvant therapy for stage III colon cancer (9). It has also been successfully combined with oxaliplatin as the capecitabine plus oxaliplatin (XELOX) regimen, which consists of a 21-day intermittent schedule of capecitabine combined with a 3-weekly dose of oxaliplatin (10,11). A pivotal phase III study (NO16966) recently demonstrated that XELOX was non-inferior in terms of efficacy to FOLFOX4 as the first-line treatment for patients with MCRC (12). The same study further showed that adding bevacizumab (Avastin®) to oxaliplatin-based chemotherapy significantly improved progression-free survival (PFS) by 20% in the first-line treatment of MCRC (13). However, most of the clinical development of these regimens has been performed in Europe and the USA, although the NO16966 study included a small number of centers in Central and Eastern Asia (12,13). It has not been clarified if XELOX with the dose and schedule applied mainly to Caucasian patients shows a similar efficacy and toxicity profile in Japanese patients. To address this issue, we conducted a Phase I/II study to evaluate the safety and efficacy of XELOX plus bevacizumab in Japanese patients with MCRC.

PATIENTS AND METHODS

Study Design

A prospective, multicenter, open-label study with a three-step design was conducted to evaluate the efficacy and safety of the commonly used dose of XELOX plus bevacizumab in Japanese patients with MCRC. The purpose of step 1 was to evaluate the initial safety of XELOX in six patients; step 2 was to evaluate the initial safety of XELOX plus bevacizumab in six patients; and step 3 was to evaluate the efficacy and safety of XELOX plus bevacizumab in 48 patients plus the six patients from step 2. The criterion for proceeding to the next phase was the occurrence of dose-limiting toxicity (DLT) in less than or equal to two of six patients. An independent review committee (IRC) was scheduled to evaluate safety immediately after the first cycle in steps 1 and 2. The previous phase I trial determined the recommended dose of the XELOX regimen (14) and DLT was defined as grade 4 neutropenia for 5 days or more, or febrile neutropenia, or grade $\geq$3 neutropenia associated with grade 3/4 complications (e.g. stomatitis, diarrhea); or grade $\geq$3 gastrointestinal toxicities, grade 3 hand-foot syndrome (HFS), grade $\geq$3 peripheral neuropathy, or any grade 4 hematological toxicity or any other clinically significant grade $\geq$3 non-hematological toxicity which did not recover within 2 days with appropriate therapy.

The study was performed in accordance with the Declaration of Helsinki and Good Clinical Practice. Written informed consent was obtained from all patients participating in this study. The protocol was approved by the independent ethics committee or institutional review board at each site.

Patients

At study enrollment, patients were required to fulfill all of the following criteria: age $\geq$20 and $\leq$74 years, Eastern Cooperative Oncology Group (EGOG) performance status of 0 or 1, life expectancy $\geq$3 months, histologically proven adenocarcinoma of the colon or rectum that was considered to be unrespectable with at least one measurable metastasis (RECIST guidelines) (15), no prior systemic chermotherapy for MCRC, no progression within 6 months of adjuvant therapy completion (if received), neutrophil count $\geq$1500/mm^3, platelet count $\geq$100 000/mm^3, hemoglobin level $\geq$9.0 g/dl, total bilirubin $\leq$1.5 times the institutional upper limit of normal (ULN), aspartate aminotransferase (AST), alanine aminotransferase and alkaline phosphatase $\leq$2.5 times ULN, creatinine $\leq$1.5 times ULN and creatinine clearance $\geq$50 ml/min. Some of the exclusion criteria were as follows: brain tumors or brain metastases, clinically detectable ascites; major surgery, open biopsy or significant traumatic injury within 4 weeks before enrollment, fine needle aspiration biopsy or central venous line placement within 1 week before enrollment, bleeding diathesis or coagulopathy, international normalized ratio $\geq$1.5 within 1 week before enrollment, non-healing bone fracture, urinary protein $\geq$1+ within 1 week before enrollment, uncontrolled hypertension or peptic ulcer, clinically significant cardiovascular disease, chronic, daily treatment with high-dose aspirin ($\geq$325 mg/day) or non-steroidal anti-inflammatory medications, or peripheral neuropathy of at least grade 1. The inclusion and exclusion criteria were almost identical to those used in the NO16966 study (12,13).

Treatment

Oxaliplatin was supplied by Yakult Honsha Co., Ltd (Tokyo, Japan) and capecitabine and bevacizumab were supplied by Chugai Pharmaceutical Co., Ltd (Tokyo, Japan). XELOX consisted of a 2-h intravenous infusion of oxaliplatin 130 mg/m^2 on day 1 plus oral capecitabine 1000 mg/m^2 twice daily for 2 weeks of a 3-week cycle. The first dose of capecitabine was given in the evening of day 1 and the last dose in the morning of day 15. Bevacizumab at a dose of 7.5 mg/kg was administered as a 30- to 90-min intravenous

infusion before oxaliplatin on day 1 of the 3-week cycle. Treatment was continued until disease progression, intolerable adverse events or withdrawal of consent.

Treatment was to be interrupted if grade 2–4 toxicities occurred. No dose modification of bevacizumab was performed. The dose of capecitabine was to be adjusted for grade 3 or 4 thrombocytopenia or neutropenia, febrile neutropenia or non-hematological toxicities of grade 2 or higher, according to a standard scheme described in detail by Blum et al. (16). The dose of oxaliplatin was to be reduced to 100 or 85 mg/m^2 if patients experienced grade 3 or 4 thrombocytopenia or neutropenia, febrile neutropenia, or grade 3 non-hematological toxicity, and for grade 3 neurosensory toxicity lasting more than 7 days, or grade 2 neurosensory toxicity persisting between cycles. For grade 3 neurosensory toxicity persisting between cycles, oxaliplatin was to be discontinued. This treatment plan was almost identical to that of the NO16966 study (12,13).

If oxaliplatin and/or bevacizumab were discontinued, treatment with the remaining components could be continued, such as capecitabine with or without bevacizumab after discontinuation of oxaliplatin, and XELOX or capecitabine after discontinuation of bevacizumab. Continuation of oxaliplatin or bevacizumab without capecitabine was not permitted.

Efficacy and Safety Evaluation

Tumor assessments with computed tomography scan were performed within 2 weeks before registration to this study and repeated every 6 weeks. Response rate was evaluated by the investigators according to RECIST version 1.0 (15). Tumor responses were confirmed by the IRC.

PFS was defined as the duration from the date of the first dose of the study drug to the date of first confirmation of disease progression as determined by the IRC, or death from any cause, and censored at the last tumor assessment if a patient withdrew before progression. Overall survival (OS) was defined as the duration from the first dose of study drug to death. Time to response was defined as the time interval from the first dose of study drug to the first detection of $\geq$30% decrease of tumor size assessed by the IRC for patients with a confirmed overall response of PR or CR. Response duration was defined as the time interval from the first detection of $\geq$30% decrease of tumor size to disease progression assessed by the IRC and censored at the last tumor assessment if a patient withdrew before progression.

Safety was assessed weekly for the first eight cycles of the treatment. Adverse events were evaluated according to the National Cancer Institute Common Terminology Criteria for Adverse Events, version 3.0 (17). All adverse events were evaluated until 28 days after the last dose of study drug.

Statistical Analysis

The primary study endpoints were safety and overall response rate (ORR) as assessed by the IRC. Secondary endpoints were PFS, OS, time to response and response duration.

Forty-eight patients were required to test the null hypothesis (P = p0 or lower) versus the alternative hypothesis (P = pA or higher) with a one-sided α-level of 2.5% and a power of 80% when the critical ORR (p0) was 35% and the expected ORR (pA) was 55%. The total number of patients recruited to receive XELOX plus bevacizumab was estimated to be 54 (6 for Step 2 and 48 for Step 3) to allow for patients who might be ineligible for efficacy evaluation.

ORRs were presented with 95% confidence interval (CI). The probabilities of time-to-event parameters were estimated using the Kaplan–Meier method with 95% CI.

RESULTS

Patient Characteristics

A total of 64 patients were enrolled between February 2006 and November 2006 from 11 centers in Japan. Six patients were enrolled in step 1 and received XELOX and 58 patients were enrolled in steps 2 and 3 and received XELOX plus bevacizumab. All patients (n = 64) were included in the safety analysis. One patient was excluded from the efficacy analysis because he received bevacizumab as part of a different clinical trial. Therefore, six patients were included in the efficacy evaluation of XELOX and 57 patients were included in the efficacy evaluation of XELOX plus bevacizumab.

The baseline demographic characteristics of the enrolled study patient population are shown in Table 1. The median age of the patients treated with XELOX was 58.5 years (range, 40–68 years) and with XELOX plus bevacizumab was 57.0 years (range, 33–74 years). ECOG performance status with XELOX was 0 in all 6 patients, and with XELOX plus bevacizumab was 0 in 50 patients and 1 in 8 patients.

Treatment Duration

In the six patients participating in step 1, the median duration of treatment was 6.5 months (range, 0.5–14 months) with a median of 8.5 treatment cycles (range, 1–17 cycles). XELOX combination therapy was administered for a median of 7.0 cycles (range, 1–17 cycles). One patient subsequently went on to receive a further 6 cycles of capecitabine monotherapy for a total of 13 cycles.

In steps 2 and 3, the median duration of treatment was 7.6 months (range, 0.1–34.8 months) with a median of 10.5 treatment cycles (range, 1–47 cycles). XELOX plus bevacizumab combination therapy was administered for a median of 9.0 cycles (range, 1–27 cycles). After discontinuation of oxaliplatin, 17 patients (29%) continued with capecitabine and bevacizumab combination therapy and received a median of 5.0 cycles (range, 1–34 cycles). Four patients (7%) received XELOX therapy for a median of 2.0 cycles

Table 1. Baseline demographic characteristics

Characteristic	XELOX ($n = 6$)		XELOX plus bevacizumab ($n = 58$)	
	No. of patients	%	No. of patients	%
Sex				
Male	5	83	40	69
Female	1	17	18	31
Age				
Median	58.5		57.0	
Range	40–68		33–74	
ECOG performance status				
0	6	100	50	86
1	0	0	8	14
Primary tumor site				
Colon	4	67	31	53
Rectum	2	33	27	47
Metastatic site				
Liver	5	83	45	78
Lung	2	33	28	48
Lymph node	0	0	27	47
Other	3	50	5	9
No. of organs involved				
1	2	33	25	43
2	4	67	21	36
3	0	0	10	17
>3	0	0	2	3
Adjuvant therapy				
Yes	1	17	8	14
No	5	83	50	86

ECOG, Eastern Cooperative Oncology Group.

(range, 1–5 cycles) during permanent or temporary discontinuation of bevacizumab.

The median relative dose intensity (ratio of dose received to dose planned) was 0.74 (range: 0.41–1.00) for capecitabine, 0.86 (range: 0.55–1.00) for oxaliplatin and 0.91 (range: 0.58–1.01) for bevacizumab.

Efficacy

At the final data cut-off date (30 June 2009), the median duration of follow-up was 32.0 months. Thirty-three patients had died of disease progression and two patients were still receiving study medication. Tumor responses (ORR, time to response, response duration and PFS) are based on the median duration of follow-up of 15.2 months.

The analysis of efficacy is shown in Table 2. The ORR (complete plus partial response) with XELOX was 67% (4/6)

Table 2. Analysis of efficacy

Endpoint	XELOX ($n = 6$)	XELOX plus bevacizumab ($n = 57$)
Median progression-free survival, months	8.3	11.0
95% confidence interval	5.8–13.8	9.6–12.5
Median overall survival, months	–	27.4
95% confidence interval	–	22.0-NC
Response rate, %	67	72
95% confidence interval	22.3–95.7	58.5–83.0
Complete response	0	2
Partial response	4	39
Stable disease	1	9
Progressive disease	0	1
Not evaluable	1	6
Median time to response, months	2.6	2.7
95% confidence interval	1.2–NC	1.5–2.8
Median response duration, months	6.4	9.7
95% confidence interval	2.8–11.3	6.7–9.9

NC, not calculated.

(95% CI: 22.3–95.7%), and with XELOX plus bevacizumab was 72% (41/57) (95% CI: 58.5–83.0%). The median PFS with XELOX plus bevacizumab was 11.0 months (95% CI: 9.6–12.5 months) (Fig. 1) and the median OS was 27.4 months (95% CI: 22.0 months–not calculated) (Fig. 2).

Eight patients (14%) treated with XELOX plus bevacizumab underwent surgery with curative intent: none experienced a serious adverse event as a result of surgery and four patients (7%) had no residual disease. The sites of resection being curative by surgery were liver ($n = 7$), lymph node ($n = 1$), cholesyst ($n = 2$) and colon primary tumor ($n = 2$).

Safety

No DLT occurred during either step 1 or step 2. All six patients treated with XELOX and 31 (53%) patients treated with XELOX plus bevacizumab discontinued study treatment because of disease progression. Ten (17%) patients withdrew from XELOX plus bevacizumab because of adverse events, which comprised dehydration and anorexia; gastric varices haemorrhage; enteritis infectious; anorexia, herpes zoster and nausea; neutropenia; AST increased and alanine aminotransferase increased; infected epidermal cyst; peripheral sensory neuropathy; epididymitis; HFS (one patient, respectively). No patient died within 28 days after study medication.

All patients ($n = 64$) experienced at least one adverse event during the study, most of which were mild to moderate

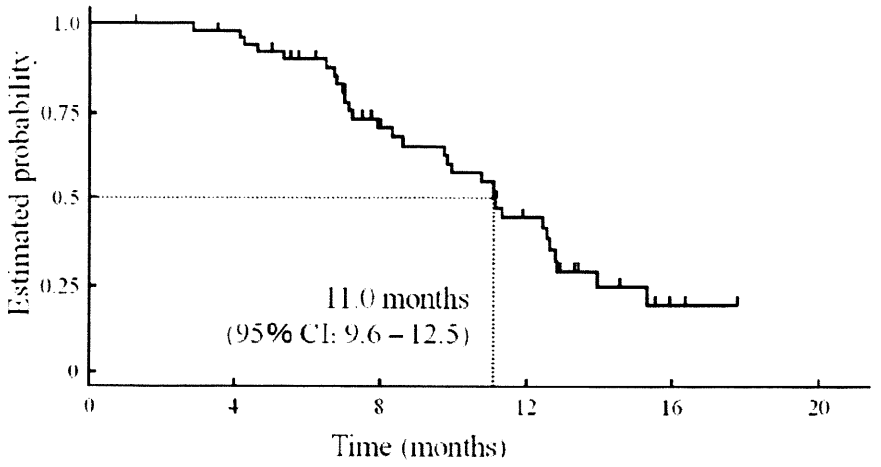

Figure 1. Progression-free survival (XELOX plus bevacizumab).

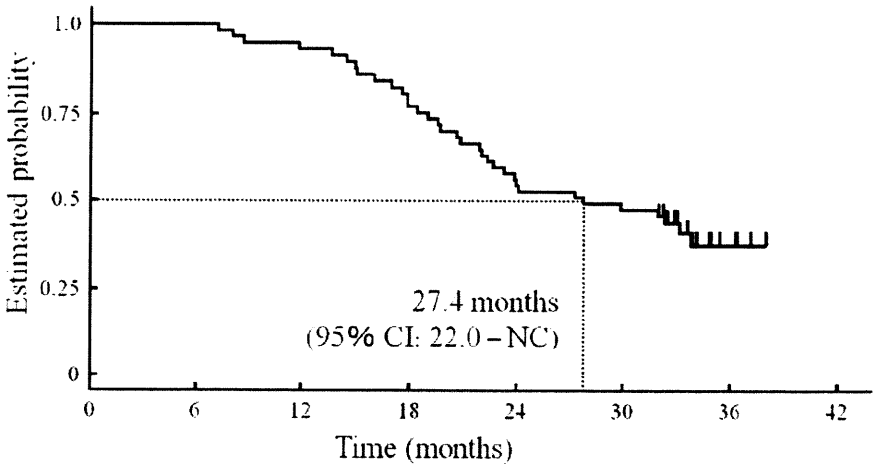

Figure 2. Overall survival (XELOX plus bevacizumab). NC, not calculated.

in severity (Table 3). The most common adverse events with XELOX plus bevacizumab were neurosensory toxicity (93%), anorexia (90%), fatigue (83%) and HFS (78%). The most common grade 3/4 adverse events were neurosensory toxicity (17%) and neutropenia (16%).

For patients receiving XELOX plus bevacizumab, dose reductions were required for capecitabine in 32 patients (55.2%); the major reasons were HFS ($n = 7$), neutropenia ($n = 6$) and diarrhea ($n = 6$). Capecitabine doses were reduced to 75% of starting dose in 18 patients and to 50% in 14 patients. Dose reductions were required for oxaliplatin in 30 patients (51.7%) due to neurosensory toxicity ($n = 15$), neutropenia ($n = 7$) and other toxicities, and in most of these patients ($n = 27$) the oxaliplatin dose was reduced to 100 mg/m^2.

DISCUSSION

In this prospective trial for Japanese patients with MCRC, XELOX plus bevacizumab achieved a high response rate of 72%, and eight patients (14%) proceeded to surgery with curative intent. The median PFS and the median OS for XELOX plus bevacizumab were 11.0 and 27.4 months, respectively.

Previous randomized or observational trials which included the XELOX plus bevacizumab regimen as first-line therapy have been conducted mainly in North America and Europe (13,18–22). The NO16966 study showed a longer PFS and OS in the XELOX plus bevacizumab arm compared with the XELOX plus placebo arm in a subgroup analysis, which reported a median PFS of 9.3 versus 7.4 months, HR = 0.77 (95% CI: 0.63–0.94, $P = 0.0026$) and a median OS of 21.6 versus 19.0 months (HR was not shown) (23,24). Furthermore, another phase III trial (CAIRO2) reported a response rate of 50.0%, a median PFS of 10.7 months and a median OS of 20.3 months in the XELOX plus bevacizumab arm (18). The patient baseline demographic characteristics of the enrolled study patient population were similar to those of previous clinical trials in Western patients, except that the proportion of rectal cancer whose prognosis is worse than

Table 3. Incidence of common adverse events

Adverse event	XELOX ($n = 6$)				XELOX plus bevacizumab ($n = 58$)			
	Grade 1–4		Grade 3–4		Grade 1–4		Grade 3–4	
	No.	%	No.	%	No.	%	No.	%
Neurosensory toxicity	6	100	1	17	54	93	10	17
Anorexia	5	83	0	0	52	90	2	3
Fatigue	4	67	0	0	48	83	3	5
Hand-foot syndrome	4	67	1	17	45	78	1	2
Nausea	6	100	0	0	43	74	0	0
Pigmentary disturbance	2	33	0	0	36	62	0	0
Stomatitis	2	33	0	0	33	57	1	2
Diarrhea	4	67	0	0	32	55	2	3
Neutropenia	3	50	0	0	30	52	9	16
Vomiting	1	17	0	0	27	47	1	2
Nose bleed	1	17	0	0	23	40	0	0
Proteinuria	0	0	0	0	19	33	3	5
Hypertension	0	0	0	0	19	33	3	5
Thrombocytopenia	2	33	1	17	13	22	4	7
Pulmonary thrombosis	0	0	0	0	1	2	1	2
Jugular vein thrombosis	0	0	0	0	1	2	0	0

that of colon cancer was higher in this study (47% versus 23–35%) (4,6–8,11,12). Thus, the efficacy data from our study compares favorably with that reported in other recently conducted studies in predominantly Western patients, although in comparing the efficacy data from 57 patients of this single arm study to those of randomized phase III trials caution should be exercised.

The administration schedule and doses selected for our study were identical to those used in the NO16966 study (12,13). The median relative dose intensity was similar with that in the XELOX plus bevacizumab arm of the NO16966 study (0.74 versus 0.73 for capecitabine, 0.86 versus 0.81 for oxaliplatin and both 0.91 for bevacizumab). The relative dose intensity was reported in another phase II trial (TREE-2) as well, a median of 0.76 for capecitabine, 0.91 for oxaliplatin and 0.96 for bevacizumab in the XELOX plus bevacizumab arm, whereas the starting dose of capecitabine was reduced to 850 mg/m^2 twice daily and the median duration of the therapy was 19 weeks in that study (14). The safety profile observed in our study was similar to that observed in previous clinical trials with Western patients, including the NO16966 study (12,13,18–22). It is notable that the incidence of grade 3/4 diarrhea was only 3%, which is considerably lower than that reported with XELOX plus bevacizumab in the previous phase II and III studies (19–21%) (12,18,19,22). A lower incidence of diarrhea has been reported in other studies of Japanese or Asian patients treated with fluoropyrimidine-based chemotherapy (25–27). In addition, clinical trials including other oral fluoropyrimidines, such as UFT, have reported lower incidence of grade 3/4 diarrhea in Japanese patients than in Western patients (9.1 versus 22.2%) (28). A reason for this regional variation remains unclear, but it is speculated that differences in dietary folate intake may be a potential explanation (29). Regarding to HFS, although the overall incidence of HFS in our study (78%) was higher than that in the XELOX plus bevacizumab arm of the NO16966 study (39%), the incidence of grade 3 HFS appeared significantly lower (2 versus 12%). The incidence of dose modification (including treatment interruption and delay) due to HFS was similar among the studies (data not shown), as well as the dose intensity of capecitabine as described above. Therefore, the difference in incidences of grade 3 HFS, unfortunately, is not well explained at this time. However, a number of factors may explain this difference. The dose modification of capecitabine due to adverse events other than HFS (e.g. neutropenia, increase of AST, fatigue, anorexia), which occurred at higher incidences in our study compared with the NO16966 study, might be one such factor (data not shown). Difference in frequency of visits could also be factor. Patients received medical examination once every week during first eight cycles in this study, resulting in the treatment interruption in the middle of first 2 weeks of a cycle in four patients among eleven patients who developed grade 2 or grade 3 HFS. Another potential reason might be differences in prophylactic administration (e.g. a moisturizer, steroid ointment, urea ointment etc.). In terms of hematologic toxicities, grade 3/4 neutropenia occurred at 16% in patients receiving XELOX plus bevacizumab in our study which was higher than in the XELOX/XELOX + placebo arm of the NO16966 study (6%) (12), whereas no febrile neutropenia was observed in any patient in our study. The difference in the incidence of grade 3/4 neutropenia may in part be derived from an increased frequency of hematological examination, which was performed once every week in this study in contrast to once every 3 weeks at day 1 in the pivotal phase III study. Known bevacizumab-specific events (i.e. coagulopathy, hypertension, bleeding) were generally mild to moderate in severity in our study, and grade 3/4 events occurred at similar or lower incidence to that reported in Western patients (13). It is concluded that XELOX plus bevacizumab is well tolerated in Japanese patients with MCRC.

Only one patient (2%) treated with XELOX plus bevacizumab experienced grade 3 HFS, compared with an incidence of 13% in a previous phase II study of capecitabine monotherapy (1250 mg/m^2 twice daily) in Japanese patients with MCRC (25). In addition, dose reduction of capecitabine due to HFS was required for less patients in our study (12.1 versus 31.7%). This may be attributable to the 20% reduced dose of capecitabine used in the XELOX regimen compared with capecitabine monotherapy.

In the present trial, six patients received only XELOX. The ORR was 67%, grade 3 adverse events developed in

three patients (one event each, respectively) and no significant safety finding was observed. XELOX without bevacizumab is a widely used regimen in a first-line setting for MCRC patients (NCCN guideline) (30). The NO16966 study demonstrated an encouraging efficacy as described above, and another phase III trial showed an ORR of 42%; PFS of 9.3 months; and median OS of 19.9 months in the XELOX arm, with a good safety profile (31). Thus, XELOX seems to be acceptable as an option for a standard regimen for MCRC in Japan, although the data provided in our study is limited to a small population.

In conclusion, in this study, XELOX plus bevacizumab was effective with manageable tolerability profile for Japanese patients with MCRC. The efficacy and safety profile of XELOX plus bevacizumab in this study was consistent with that observed in Western patients, whereas showing a notably lower incidence of diarrhea. Moreover, the XELOX regimen requires only one visit per 3-week cycle for a 2- or 3-h infusion, which may provide a marked advantage over the FOLFOX regimen in terms of the convenience for both patients and clinical staff. Therefore, XELOX plus bevacizumab may be considered as a possible standard treatment for Japanese patients with MCRC.

Acknowledgements

We are indebted to Dr Yuh Sakata, Dr Ichinosuke Hyodo and Dr Kunihisa Miyakawa for their help in the assessment of efficacy and evaluation of safety. We are also grateful to Dr Tetsuo Taguchi, Dr Nagahiro Saijo and Dr Atsushi Ohtsu for supporting the study.

Funding

This work was supported by Chugai Pharmaceutical Co. Ltd and Yakult Honsha Co. Ltd.

Conflict of interest statement

None declared.

References

1. Jemal A, Tiwari RC, Murray T, Ghafoor A, Samuels A, Ward E, et al. American Cancer Society, Cancer statistics 2004. *CA Cancer J Clin* 2004;54:8–29.
2. Parkin DM. Global cancer statistics in the year 2000. *Lancet Oncol* 2001;2:533–43.
3. Cancer Statistics in Japan Editorial Board. *Cancer Statistics in Japan 2009. Foundation for Promotion of Cancer Research*; 2009.
4. de Gramont A, Figer A, Seymour M, Homerin M, Hmissi A, Cassidy J, et al. Leucovorin and fluorouracil with or without oxaliplatin as first-line treatment in advanced colorectal cancer. *J Clin Oncol* 2000;18:2938–47.
5. Goldberg RM, Morton RF, Sargent DJ, Fuchs CS, Ramanathan RK, Williamson SK, et al. A randomized controlled trial of fluorouracil plus leucovorin, irinotecan, and oxaliplatin combinations in patients with previously untreated metastatic colorectal cancer. *J Clin Oncol* 2004;22:23–30.
6. VanCutsem E, Twelves C, Cassidy J, Allman D, Bajetta E, Boyer M, et al. Oral capecitabine compared with intravenous fluorouracil plus leucovorin in patients with metastatic colorectal cancer: Results of a large phase III study. *J Clin Oncol* 2001;19:4097–106.
7. Van Cutsem E, Hoff PM, Harper P, Bukowski RM, Cunningham D, Dufour P, et al. Oral capecitabine vs intravenous 5-fluorouracil and leucovorin: integrated efficacy data and novel analyses from two large, randomized, phase III trials. *Br J Cancer* 2004;90:1190–7.
8. Hoff PM, Ansari R, Batist G, Cox J, Kocha W, Kuperminc M, et al. Comparison of oral capecitabine versus intravenous fluorouracil plus leucovorin as first-line treatment in 605 patients with metastatic colorectal cancer: results of a randomized phase III study. *J Clin Oncol* 2001;19:2282–92.
9. Twelves C, Wong A, Nowacki MP, Abt M, Burris H, 3rd, Carrato A, et al. Capecitabine as adjuvant treatment for stage III colon cancer. *N Engl J Med* 2005;352:2696–704.
10. Cassidy J, Tabernero J, Twelves C, Brunet R, Butts C, Conroy T, et al. XELOX (capecitabine plus oxaliplatin): Active first-line therapy for patients with metastatic colorectal cancer. *J Clin Oncol* 2004;22:2084–91.
11. Rothenberg ML, Cox JV, Butts C, Navarro M, Bang YJ, Goel R, et al. Capecitabine plus oxaliplatin (XELOX) versus 5-fluorouracil/folinic acid plus oxaliplatin (FOLFOX-4) as second-line therapy in metastatic colorectal cancer: a randomized phase III noninferiority study. *Ann Oncol* 2008;19:1720–6.
12. Cassidy J, Clarke S, Díaz-Rubio E, Scheithauer W, Figer A, Wong R, et al. Randomized phase III study of capecitabine plus oxaliplatin compared with fluorouracil/folinic acid plus oxaliplatin as first-line therapy for metastatic colorectal cancer. *J Clin Oncol* 2008;26:2006–12.
13. Saltz L, Clarke S, Díaz-Rubio E, Scheithauer W, Figer A, Wong R, et al. Bevacizumab in combination with oxaliplatin-based chemotherapy as first-line therapy in metastatic colorectal cancer: a randomized phase III study. *J Clin Oncol* 2008;26:2013–9.
14. Díaz-Rubio E, Evans TR, Tabemero J, Cassidy J, Sastre J, Eatock M, et al. Capecitabine (Xeloda®) in combination with oxaliplatin: a phase I, dose-escalation study in patients with advanced or metastatic solid tumors. *Ann Oncol* 2002;13:558–65.
15. Therasse P, Arbuck S, Eisenhauer E, Wanders J, Kaplan R, Rubinstein L, et al. New guidelines to evaluate the response to treatment in solid tumors. *J Natl Cancer Inst* 2000;92:205–16.
16. Blum JL, Jones SE, Buzdar AU, et al. Multicenter phase II study of capecitabine in paclitaxel-refractory metastatic breast cancer. *J Clin Oncol* 1999;17:485–93.
17. National Cancer Institute-Common Terminology Criteria for Adverse Events (NCI-CTC Version 3.0, 31 March 2003).
18. Tol J, Koopman M, Cats A, Rodenburg CJ, Creemers GJ, Schrama JG, et al. Chemotherapy, bevacizumab, and cetuximab in metastatic colorectal cancer. *N Engl J Med* 2009;360:563–72.
19. Hochster HS, Hart LL, Ramanathan RK, Childs BH, Hainsworth JD, Cohn AL, et al. Safety and efficacy of oxaliplatin and fluoropyrimidine regimens with or without bevacizumab as first-line treatment of metastatic colorectal cancer: results of the TREE Study. *J Clin Oncol* 2008;26:3523–2539.
20. Berry SR, Van Cutsem E, Kretzschmar A, Michael M, Rivera F, DiBartolomeo M, et al. Final efficacy results for bevacizumab plus standard first-line chemotherapies in patients with metastatic colorectal cancer: First BEAT. *J Clin Oncol* 2008;26(Suppl.; abstr 4025).
21. Kozloff M, Hainsworth J, Badarinath S, Cohn A, Flynn PJ, Dong W, et al. Survival of patients (pts) with mCRC treated with bevacizumab in combination with chemotherapy: Results from the BRiTE registry. *Presented at the ASCO GI Cancers Symposium, 19–21 January* 2007 (abstr 375).
22. Reinacher-Schick AC, Kubicka S, Freier W, Arnold D, Dietrich G, Geissler M, et al. Activity of the combination of bevacizumab (Bev) with capecitabine/irinotecan (CapIri/Bev) or capecitabine/oxaliplatin (CapOx/Bev) in advanced colorectal cancer (ACRC): a randomized phase II study of the AIO Colorectal Study Group (AIO trial 0604). *J Clin Oncol* 2008;26(Suppl.; abstr 4030)
23. Saltz L, Clarke S, Diaz-Rubio E, Scheithauer W, Figer A, Wong R, et al. Bevacizumab (Bev) in combination with XELOX or FOLFOX4 : Efficacy results from XELOX-1/NO16966, a randomized phase III trial

in the first-line treatment of metastatic colorectal cancer (MCRC). *Presented at the ASCO GI Cancers Symposium* 2007 (abstr 238).
24. Cassidy J, Clarke S, Díaz-Rubio E, Scheithauer W, Figer A, Wong R, et al. XELOX-1/NO16966, a randomized phase III trial of first-line XELOX compared with FOLFOX4 for patients with metastatic colorectal cancer (MCRC); Updated survival and tolerability results. *Presented at the ASCO GI Cancers Symposium* 2009; (abstr 382).
25. Hyodo I, Shirao K, Doi T, Hatake K, Arai Y, Yamaguchi K, et al. A phase II study of the global dose and schedule of capecitabine in Japanese patients with metastatic colorectal cancer. *Jpn J Clin Oncol* 2006;36:410–7.
26. Rothenberg ML, Saltz L, Cunningham D, Cassidy J, Diaz-Rubio E, Scheithauer W, et al. Tolerability of fluoropyrimidines in combination with oxaliplatin appears to differ by region. *Presented at the ASCO GI Cancers Symposium, 25–27 January* 2008 (abstr 456).
27. Yoshino T, Boku N, Onozawa Y, Hironaka S, Fukutomi A, Yamaguchi Y, et al. Efficacy and safety of an irinotecan plus bolus 5-fluorouracil and L-leucovorin regimen for metastatic colorectal cancer in Japanese patients: experience in a single institution in Japan. *Jpn J Clin Oncol* 2007;37:686–91.
28. Shirao K, Hoff P, Ohtsu A, Loehrer P, Hyodo I, Wadler S, et al. Comparison of the efficacy, toxicity, and pharmacokinetics of a uracil/tegafur (UFT) plus oral leucovorin (LV) regimen between Japanese and American patients with advanced colorectal cancer: joint United States and Japan study of UFT/LV. *J Clin Oncol* 2004;22:3466–74.
29. Haller DG, Cassidy J, Clarke SJ, Cunningham D, Van Cutsem E, Hoff PM, et al. Potential regional differences for the tolerability profiles of fluoropyrimidines. *J Clin Oncol* 2008;26:2118–23.
30. NCCN Clinical Practice Guidelines in Oncology, colon cancer, v.3. 2009.
31. Ducreux M, Bennouna J, Hebber M, Ychou M, Lledo G, Conroy T, et al. Efficacy and safety findings from a randomized phase III study of capecitabine (X) + oxaliplatin (O) (XELOX) vs. infusional 5-FU/LV + O (FOLFOX-6) for metastatic colorectal cancer (MCRC). *J Clin Oncol* 2007;25(Suppl.; abstr 4029).

Appendix

The following investigators cared for the patients in this study: Kuniaki Shirao (Oita University, Faculty of Medicine, Yufu, Oita) and Takashi Sekikawa (Toyosu Hospital, Showa University School of Medicine, Tokyo).

Highlighted paper selected by Editor-in-Chief

Nucleolin on the Cell Surface as a New Molecular Target for Gastric Cancer Treatment

Tatsuro WATANABE,[a,b] Kazuya HIRANO,[c] Atsushi TAKAHASHI,[a,b] Kensei YAMAGUCHI,[d] Masatoshi BEPPU,[c] Hirota FUJIKI,[c] and Masami SUGANUMA*[,a]

[a] *Research Institute for Clinical Oncology, Saitama Cancer Center;* [d] *Hospital, Saitama Cancer Center; Ina, Kitaadachi-gun, Saitama 362–0806, Japan:* [b] *Graduate School of Science and Engineering, Saitama University; 255 Shimo-Okubo, Sakura-ku, Saitama 338–8570, Japan:* [c] *School of Pharmacy, Tokyo University of Pharmacy and Life Science; 1432–1 Horinouchi, Hachioji, Tokyo 192–0392, Japan: and* [c] *Faculty of Pharmaceutical Sciences, Tokushima Bunri University; 180 Nishihamaboji, Yamashirocho, Tokushima 770–8514, Japan.*

Received February 9, 2010; accepted February 18, 2010; published online February 19, 2010

Nucleolin is an abundant non-ribosomal protein found in nucleolus and a major component of silver-stained nucleolar organizer region (AgNOR), a histopathological marker of cancer which is highly elevated in cancer cells. We recently reported that nucleolin on the cell surface of mouse gastric cancer cells acts as a receptor for tumor necrosis factor-α-inducing protein (Tipα), a new carcinogenic factor of *Helicobacter pylori*. In this study, we first examined the localization of nucleolin on cell surface of five gastric cancer cell lines by cell fractionation and flow cytometry: We found that large amounts of nucleolin were present on surface of MKN-45, KATOIII, MKN-74, and AGS cells, with smaller amounts on surface of MKN-1 cells. The membrane fraction of normal epithelial cells of mouse glandular stomach did not contain much nucleolin, suggesting that translocation of nucleolin to the cell surface occurs during carcinogenesis, making for easier binding with Tipα. AS1411, a nucleolin targeted DNA aptamer, inhibited growth of gastric cancer cell lines in this order of potency: MKN-45>KATOIII>AGS>MKN-74=MKN-1, associated with induction of S-phase cell cycle arrest. Fluorescein isothiocyanate (FITC)-AS1411 was more rapidly incorporated into MKN-45 and AGS than into MKN-1 cells, based on varying amounts of cell surface nucleolin. We think that AS1411 first binds to nucleolin on the cell surface and that the binding complex is then incorporated into the cells. All results indicate that nucleolin on the cell surface is a new and promising therapeutic target for treatment of gastric cancer.

Key words nucleolin; cell-surface localization; gastric cancer; DNA aptamer; *Helicobacter pylori*

Nucleolin is a well-known major non-ribosomal protein consisting of 710 amino acids in nucleolus: biochemically it is a ubiquitous phosphoprotein which serves as regulator of ribosomal biogenesis and maturation, including the control of ribosomal DNA (rDNA) transcription, pre-ribosome packaging, and organization of nucleolar chromatin.[1,2] We recently reported that TNF-α inducing protein (Tipα), a new carcinogenic factor (molecular weight of 19 kDa) which is transcribed from the *TNF-α inducing protein* (*Tipα*) gene in the genome of *Helicobacter pylori* (*H. pylori*) strain 26695, binds to nucleolin on the cell surface of mouse gastric cancer cell line MGT-40[3—5]: This finding provided a new mechanistic insight into gastric cancer development with Tipα mediated through nucleolin.

Looking at the unique features of nucleolin in carcinogenesis, it has been reported that the amount of nucleolin is highly elevated in rapidly proliferating cells, such as cancer cell lines, and that nucleolin is a major component of the silver-stained nucleolar organizer region (AgNOR), which is also elevated in cancer cells compared with normal or premalignant cells.[2,6,7] The localization of nucleolin on the cell surface of gastric cancer cell lines attracted our attention because nucleolin had been mainly reported to be present in nucleoli: We discovered that significant amounts of nucleolin are present on the cell surface of gastric cancer cell lines, as determined by cell fractionation method and flow cytometry analysis with anti-nucleolin antibody.

Since cell surface nucleolin serves as a receptor for various ligands, including midkine, lactoferrin, endostatin, and human immunodeficiency virus (HIV) particles, it is possible to regulate the cell growth by either a promoting ligand, like midkine, a cytokine regulating cell proliferation and differentiation, or inhibiting ligands, such as lactoferrin and endostatin.[8—11] Considering our study of nucleolin on the cell surface, we think that a ligand with anticancer activity can be used to inhibit the growth of gastric cancer cells.

The well-investigated anti-cancer aptamer named AS1411 is a DNA aptamer of 26-mer unmodified guanine-rich oligonucleotide; it specifically binds to nucleolin, resulting in inhibitions of nucleolin function and cancer cell growth *in vitro* and *in vivo*.[12,13] Since AS1411 is now in Phase II clinical trials as treatment for acute myeloid leukemia and renal cell carcinoma, we think it is worthwhile to study the effects of AS1411 on inhibition of cell growth and cell cycle regulation in gastric cancer cell lines. This manuscript is the first report that the amount of nucleolin is clearly elevated on the cell surface of gastric cancer cell lines, but not in normal mouse glandular stomach, and that AS1411 inhibits growth of gastric cancer cells probably mediated through cell surface nucleolin before it is incorporated into the cells. All the results indicate that nucleolin on the cell surface is a new molecular target for treatment of gastric cancer in humans.

MATERIALS AND METHODS

Cell Lines and Cell Culture Conditions Five human gastric cancer cell lines were used: MKN-1 (adenosquamous carcinoma), MKN-45 (poorly differentiated adenocarcinoma), MKN-74 (moderately differentiated adenocarcinoma), AGS (adenocarcinoma) and KATOIII (signet ring cell carci-

* To whom correspondence should be addressed. e-mail: masami@cancer-c.pref.saitama.jp

noma) were grown in RPMI 1640 medium with 10% fetal bovine serum (JRH Bioscience, KS, U.S.A.). Mouse gastric cancer cell line MGT-40 was maintained in Dulbecco's modified Eagle's medium (DMEM) with 10% fetal bovine serum (Bioserum, Victoria, Australia) and MITO+ serum extender (Becton, Dickinson and Company, CA, U.S.A.), as described previously.[14]

Materials Anti-nucleolin antibody (anti-NUC295) was raised in rabbits by immunizing a syntheic peptide of 8 amino acids (from 295 to 302) of nucleolin, as described previously.[15] Anti-lamin B and Anti-HSP90 antibodies were purchased from Santa Cruz Biotethnology (CA, U.S.A.). Anti-caveolin 2 antibody was from BD Transduction Laboratories (CA, U.S.A.). AS1411 with sequence 5′-d(GGTGGTGGTGGTTGTGGTGGTGGTGG)-3′, 5′-fluorescein isothiocyanate (FITC)-AS1411 and cytosine rich oligonucleotide (CRO) with sequence 5′-d(CCTCCTCCTC-CTTCTCCTCCTCCTCC)-3′ were synthesized by Sigma-Aldrich Japan (Tokyo, Japan).[13] Each oligonucleotide was dissolved in the Tris–EDTA (TE) buffer, heated at 88 °C for 10 min, and then gradually cooled to room temperature to form G-quartet structure.

Cell Fractionation and Western Blotting Homogenates of MKN-1, MKN-45, MKN-74, AGS, KATOIII, and MGT-40 cells, and of mucosa of glandular stomach of Balb/c mice (Clea Japan, Tokyo, Japan), were fractionated into membrane, cytosol, and nuclei using Qptroteome cell compartment kit (Qiagen), according to the manufacturer's instruction. Each fraction was subjected to 12% sodium dodecyl sulfate-polyacrylamide gel electrophoresis (SDS-PAGE) and subjected to Western blotting using anti-nucleolin, anti-caveolin 2 (for membrane), anti-HSP90 (a marker for cytosol), or anti-lamin B antibody (for nuclei).

Flow Cytometry Analysis MKN-1, MKN-45, MKN-74, AGS or KATOIII cells (1×10^6 cells/ml) in phosphate buffered saline (PBS) were incubated with 2 μg/ml anti-NUC295 antibody and 10 μg/ml Alexa Fluor 488-conjugated goat anti-rabbit immunoglobulin G (IgG) (Invitrogen, CA, U.S.A.) on ice for 30 min. The cells were fixed with PBS containing 2% paraformaldehyde.[15] Fluorescence intensity of each cell line was analyzed by flow cytometry (Epics XL, Beckman Coulter, CA, U.S.A.).

Cell Viability Assay MKN-1, MKN-74 or AGS cells (1×10^3 cells per well), and MKN-45 or KATOIII cells (3×10^3 cells per well) were seeded in 96-well microculture plates, and were treated with AS1411 or CRO at concentrations from 0.15 to 20 μM at 37 °C for 4 d. The number of viable cells was determined by 3-[4,5-dimethylthiazol-2-yl]-2,5-diphenyltetrazolium bromide (MTT) assay.[16] The absorbance of non-treated cells was expressed as 100%. The experiments were conducted in triplicate and the results are the means of two independent experiments.

Immunocytochemistry MKN-45 cells were stained with anti-nucleolin antibody (anti-NUC295) in non-permeabilized condition: they were incubated with 40 μg/ml anti-NUC295 for 2 h in the culture medium containing 25 mM NaN_3 at 37 °C. After fixation with 95% methanol containing 5% acetic acid, cells were treated with Alexa Fluor 488-conjugated goat anti-rabbit IgG (Invitrogen) and 4′,6-diamidino-2-phenylindole (DAPI), and examined by fluorescent microscope (BIOREVO BZ-9000, Keyence, Osaka, Japan). MKN-1 and AGS cells were incubated with 15 μM FITC-AS1411 at 37 °C for 2 h, then fixed with 95% methanol containing 5% acetic acid. The cells were treated with 10 μg/ml anti-NUC295 and stained with phycoerythrin (PE)-conjugated goat anti-rabbit IgG (Invitrogen) and DAPI.

Cell Cycle Analysis Cell cycle was examined using flow cytometry of propidium iodide (PI)-stained cells as described previously.[17] MKN-1, MKN-45 or AGS cells were treated with 5 μM AS1411 for 24 h. After fixation with ice-cold 70% ethanol for 30 min at 4 °C, cells were stained with 50 μg/ml PI.[17] DNA contents of about 10000 cells were measured by flow cytometer (Epics XL, Beckman Coulter).

Statistical Analysis The data were compared using Student's *t* test.

RESULTS

Localization of Nucleolin in the Membrane of Human Gastric Cancer Cell Lines To investigate the localization of nucleolin in gastric cancer cell lines, we used five cell lines, MKN-1, MKN-45, MKN-74, AGS, and KATOIII. The cells were fractionated into membrane, cytosolic and nuclear fractions, each of which was subjected to SDS-PAGE and further immunoblotted with anti-nucleolin antibody. In this experiment, the three polypeptide bands that reacted with anti-nucleolin antibody in the membrane fraction had molecular weights of 107, 98, and 81 kDa, similar to those of the nuclear fraction of MKN-45, MKN-74, AGS, and KATOIII cell lines (Fig. 1A). It is important to note that the amounts of nucleolin with 107 kDa in the membrane fractions were almost the same as those of the nuclear fractions in these four gastric cancer cell lines. However, MKN-1 cell line contained smaller amounts of nucleolin in the membrane fraction compared with those of the nuclear fraction (Fig. 1A). Nucleolin bands with 107 kDa in both the membrane and nuclear fractions were derived from the full length of nucleolin, and we observed its degradation fragments (98, 81 kDa) due to its unstable nature and, in part, its auto-proteolysis.[1,2] From the results, we concluded that large amounts of nucleolin were present in the membrane fractions of four gastric cancer cell lines, MKN-45, MKN-74, AGS, and KATOIII, with smaller amounts found in MKN-1, although all five gastric cancer cell lines contained similar amounts of nucleolin in the whole cell lysates (Fig. 1B).

To understand the significance of the nucleolin in membrane fraction of gastric cancer cells, we determined the localization of nucleolin in the normal epithelial cells of mouse glandular stomach by cell fractionation, and compared this with that of mouse gastric cancer cell line MGT-40. Figure 1C shows that the membrane fractions of normal glandular stomach of two different mice contained less than 1% of the nucleolin in the nuclear fraction, and that the amounts of nucleolin in the nuclear fraction of mouse glandular stomach were much lower than those in MGT-40 cells, suggesting a link between smaller amounts of nucleolin in the membrane fraction and a non-malignant status. Based on these results, we think that the normal epithelial cells of mouse glandular stomach do not contain significant amounts of nucleolin in the membrane fraction.

Presence of Nucleolin on the Cell Surface The localization of nucleolin on the cell surface was determined by

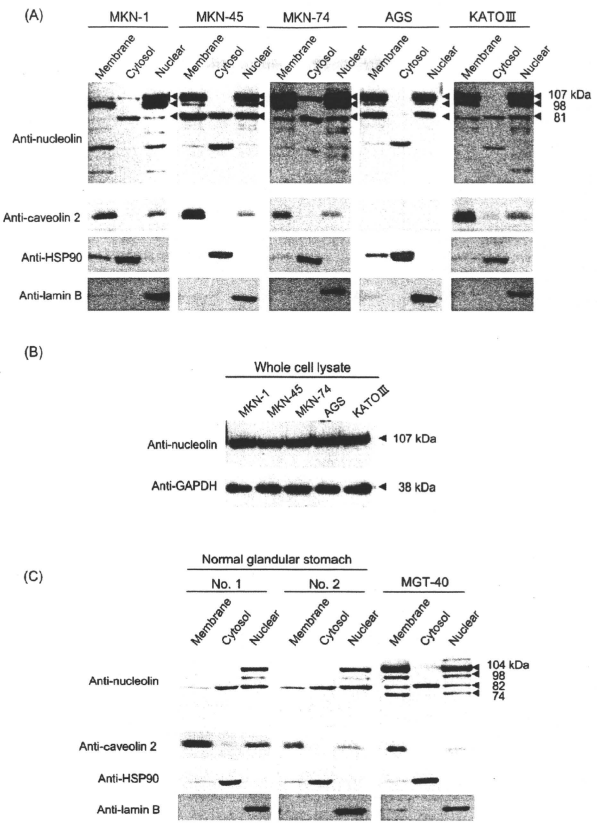

Fig. 1. Localization of Nucleolin in the Membrane Fraction of Human Gastric Cancer Cell Lines

(A) Subcellular localization of nucleolin in 5 human gastric cancer cell lines analyzed by cell fractionation. After fractionation into membrane, cytosolic and nuclear fractions, each fraction was immunoblotted with anti-nucleolin antibody or antibodies of caveolin 2 for membrane, HSP90 for cytosol and lamin B for nuclei. (B) The levels of total nucleolin in 5 human gastric cancer cell lines. (C) Subcellular localization of nucleolin in the normal epithelial cells of mouse glandular stomach. Homogenates of mucosa of glandular stomach obtained from two different mice (No. 1, 2) and mouse gastric cancer cell line (MGT-40) were examined.

flow cytometry with anti-nucleolin antibody (anti-NUC295). In this experiment, gastric cancer cell lines were incubated with anti-NUC295 and Alexa Fluor 488-labeled anti-rabbit IgG. Figure 2A shows that the fluorescent peaks of MKN-45, MKN-74, AGS and KATOIII cells dramatically shifted from basal fluorescence, when treated with pre-immune serum as a control to high fluorescence, when treated with anti-NUC295, whereas MKN-1 cells with smaller amounts of nucleolin in the membrane fraction showed a slight but significant sift of the fluorescent peak. These results strongly supported the aforementioned results of cell fractionation.

The localization of nucleolin on the cell surface of gastric cancer cell lines was confirmed by immunocytochemical analysis with anti-NUC295 in non-permeabilized conditions. MKN-45 cells were first incubated with anti-NUC295 before fixation of cells, and stained with Alexa Fluor 488-labeled anti-rabbit IgG. Nucleolin was visualized on the membrane of MKN-45 cells (Fig. 2B). All the results clearly demonstrated that nucleolin is present on the cell surface of gastric cancer cells, and that the amounts of nucleolin on the cell surface vary among cell lines.

Growth Inhibition of Gastric Cancer Cell Lines with a DNA Aptamer, AS 1411 Since AS1411, a DNA aptamer, is reported to directly bind to nucleolin,[12] in this experiment we studied the inhibitory effects on cell growth of gastric cancer cell lines with AS1411 of 26-mer guanine-rich oligonucleotide, compared with CRO of 26-mer cytosine-rich oligonucleotide as a control. AS1411 was added to culture

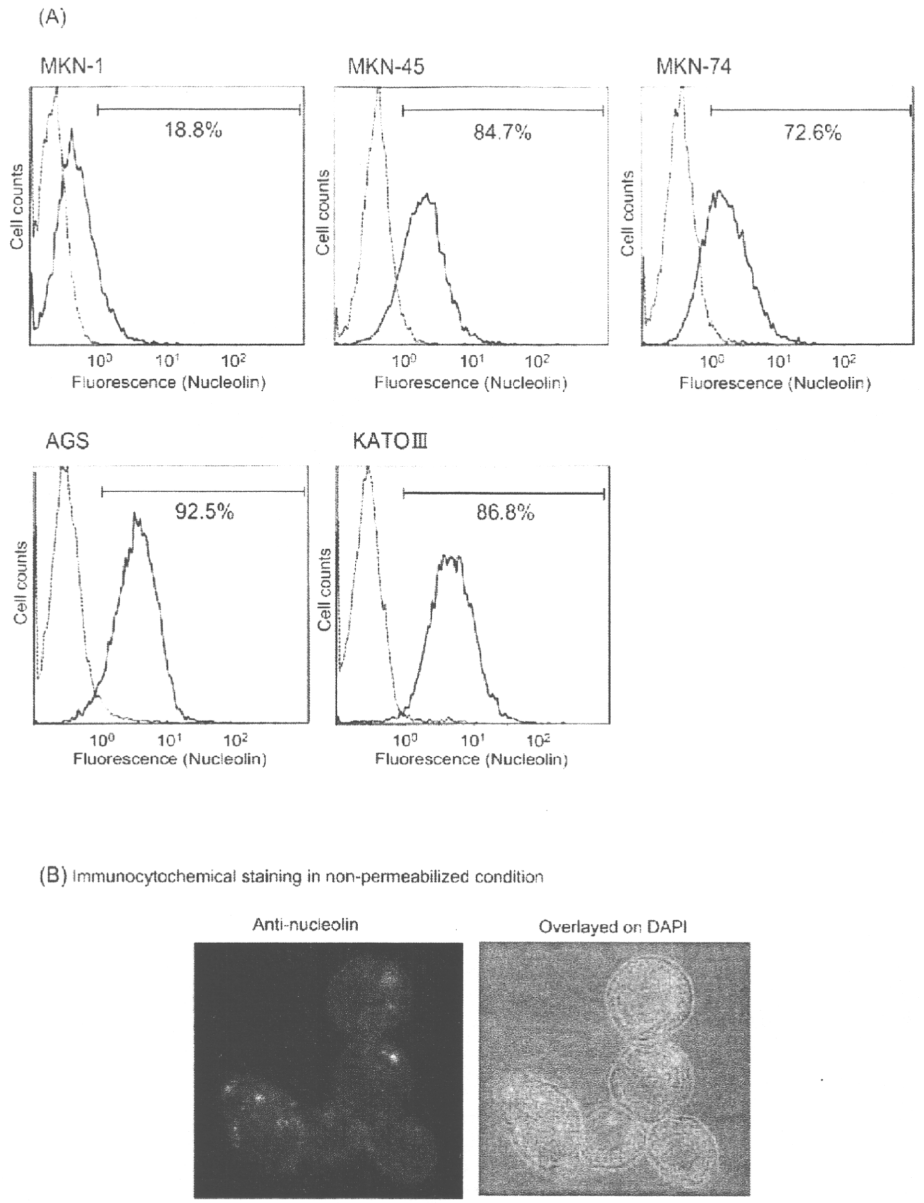

Fig. 2. Presence of Nucleolin on the Cell Surface of Human Gastric Cancer Cells

(A) Detection of nucleolin on cell surface by flow cytometry. MKN-1, MKN-45, MKN-74, AGS and KATOIII cells were incubated with anti-NUC295 (Anti-NUC295) or with pre-immune serum (pre-serum) in the presence of Alexa Fluor 488-conjugated goat anti-rabbit IgG on ice for 30 min. (B) Detection of nucleolin on cell surface by immunocytochemistry in non-permeabilized condition. MKN-45 cells were stained with anti-NUC 295 as described in Materials and Methods.

medium without any transfection reagent, and then incubated for 4 d. Figure 3 shows that AS1411 dose-dependently inhibited the cell growth of four gastric cancer cell lines, but that CRO did not show any growth inhibition. The IC_{50} values for growth inhibition with AS1411 were MKN-45 (2.3 μM)> KATOIII (9.5 μM)>AGS (10.0 μM)>MKN-74 (>20.0 μM)= MKN-1 (>20.0 μM) in order of potency. It is interesting to note that MKN-1 cells with less nucleolin on the cell surface showed similarly low responses to AS1411 and MKN-74 cells with large amounts of nucleolin, suggesting some very complex conditions.

To understand the inhibitory mechanisms of AS1411 on the growth of gastric cancer cell lines, we determined the cell cycle regulation of both MKN-1 cells with low response to AS1411, and MKN-45 cells with high response, by flow cytometory 1 d after treatment with AS1411. Treatment of MKN-45 cells with AS1411 significantly increased cells of S phase from 14.4±12.4 to 79.8±4.0%, but MKN-1 cells treated with AS1411 induced a smaller increase in cells of S phase from 17.3±2.9 to 32.9±5.0%. CRO did not induce any effects on the cell cycle of either cell lines (Fig. 4). The results suggest that the nucleolin-targeted DNA aptamer induced S-phase cell cycle arrest in MKN-45 and MKN-1 cell lines by inhibition of *de novo* DNA synthesis.

Incorporation of AS1411 into Cells with Nucleolin on the Cell Surface We studied the correlation between large amounts of nucleolin on the cell surface and incorporation of AS1411 into the gastric cancer cell lines associated with anticancer activity. The incorporation of fluorescence-labeled AS1411 (FITC-AS1411) into the cells was determined by

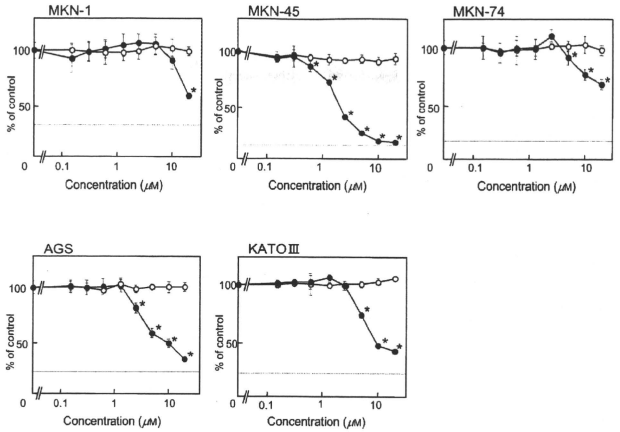

Fig. 3. Growth Inhibition of Human Gastric Cancer Cell Lines with DNA Aptamer, AS1411

The cells were incubated with AS1411 (●) or CRO (○) at concentrations from 0.15 to 20 μM for 4 d at 37 °C, then examined by MTT assay. The absorbance of non-treated cells is expressed as 100%. The dotted line indicates the cell counts before treatment with oligonucleotides. Bars indicate standard deviation. * $p<0.01$ *vs.* non-treated cells.

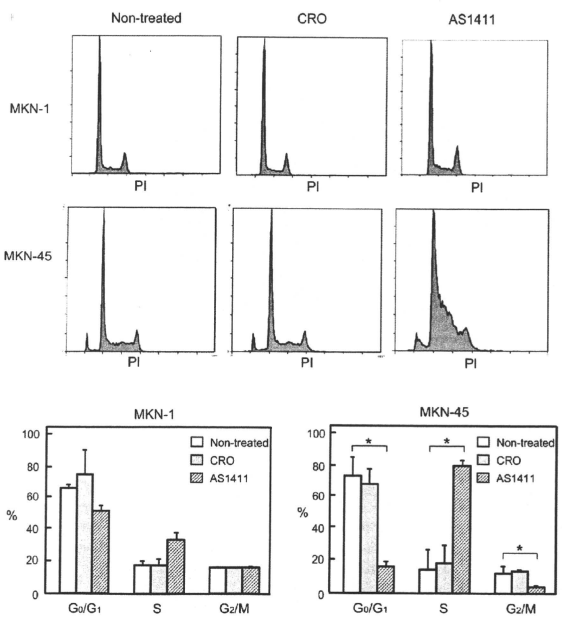

Fig. 4. S-phase Arrest of MKN-1 and MKN-45 Cells Induced by Treatment with AS1411

MKN-1 and MKN-45 cells were incubated with AS1411 or CRO at a concentration of 5 μM for 24 h at 37 °C. Cell cycle was examined by flow cytometry of PI-stained cells. * $p<0.01$ *vs.* non-treated cells.

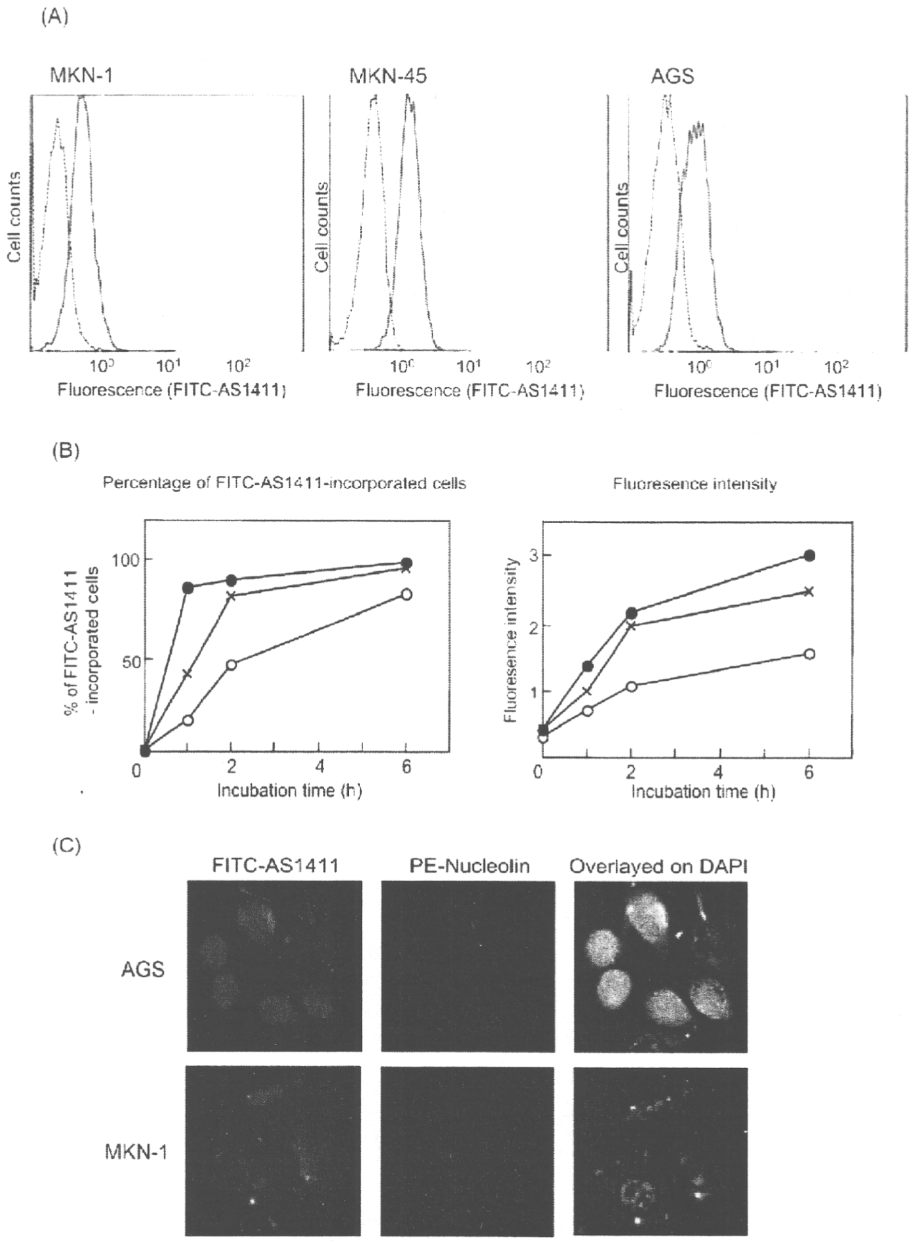

Fig. 5. Incorporation of FITC-AS1411 into Human Gastric Cancer Cells

(A) Incorporation of FITC-AS1411 into cells was measured by flow cytometry. The cells were incubated with FITC-AS1411 at a concentration of 5 μM for 1 (red line) to 6 h (green line), and subjected to flow cytometry analysis. (B) The percentage of FITC positive cells (more than 10^0) was based on FITC-AS1411 incorporated cells and the means of fluorecense intensity (FI) indicate relative levels of incorporated FITC-AS1411 into MKN-1 (○), MKN-45 (●), and AGS cells (×). (C) Incorporation of FITC-AS1411 into cells was measured by immunocytochemistry. The cells were incubated with 15 μM FITC-AS1411 for 2 h. Nucleolin was stained with anti-NUC295 and PE-labeled anti-rabbit IgG, as described in Materials and Methods.

flow cytometry (Fig. 5A). FITC-AS1411 was rapidly incorporated into MKN-45 and AGS cells with large amounts of nucleolin on the cell surface: almost 100% of the incorporated cells within 2 h. In contrast, FITC-AS1411 was gradually incorporated into MKN-1 cells with smaller amounts of nucleolin on the cell surface (Fig. 5B). The relative levels of the FITC-AS1411 incorporated into AGS and MKN-45 cells were 2—2.5 times higher than those in MKN-1 cells within 6 h after incubation (Fig. 5B). The incorporation of FITC-AS1411 into AGS and MKN-1 cells was examined by immunocytochemistry after 2 h of incubation with 15 μM: FITC-AS1411 was incorporated into both AGS and MKN-1 cells, and was colocalized with nucleolin in the cytosol and nucleolei in the cells. Fluorescence intensity of AS1411 in AGS cells seems to be much higher than that in MKN-1 cells (Fig. 5C). The direct binding of AS1411 to nucleolin on the cell surface of gastric cancer cells and its association with inhibition of cancer cell growth opens up a new strategy for screening of promising therapeutic and preventive agents for gastric cancer in humans.

DISCUSSION

In the light of our evidence that proinflammatory cytokines, such as TNF-α and IL-1 are endogenous tumor promoters, we first found Tipα as a new carcinogenic factor of *H.*

pylori.[4,18,19] Since Tipα is incorporated into the cells not mediated through Type IV secretion system of *H. pylori*, Tipα is different from CagA or urease. We recently reported the direct interaction of Tipα with nucleolin on the cell surface of MGT-40 cells, although nucleolin is predominantly present in the nucleoli.[3] The direct binding of Tipα to nucleolin induces incorporation of the binding complex into the cells, which results in cancer development. The presence of nucleolin on the cell surface seems to be an important factor in carcinogenesis, since the membrane fraction of normal epithelial cells in mouse glandular stomach does not contain much nucleolin. The results allowed us to find out whether the presence of nucleolin in the membrane fraction is a general feature of gastric cancer cells. This paper discusses the significance of nucleolin on the cell surface in carcinogenesis.

The presence of nucleolin on the cell surface is highly indicative, because nucleolin was found on the cell surface in various cancer cell lines including liver, breast, kidney, lung, colon and uterus, and in melanoma.[1,13,20,21] Moreover, we recently found that the levels of nucelolin on the cell surface in Bhas 42 (v-H-*ras* transfected BALB/3T3) cells, which are used as so-called initiated cells in the experiments, is significantly higher than in normal BALB/3T3 cells, suggesting that the activation of Ras signaling induces translocation of nucleolin from the nuclear fraction to the membrane fraction (our unpublished data). If this is so, the initiation stage may result in a hospitable cancer microenvironment for Tipα of *H. pylori*. Further study on the expression levels of nucleolin and the translocation of nucleolin to the cell surface will certainly provide new insights into the mechanisms of gastric cancer development. Since CD44 positive cells were recently reported to be possible tumor initiating cells or stem cells of gastric cancer,[22] it is definitely worth studying the amounts of nucleolin on the cell surface of CD44 positive cells.

In spite of the fact that nucleolin does not have a hydrophobic transmembrane domain, which most membrane proteins have, nucleolin is translocated from the endoplasmic reticulum and Golgi apparatus to the cell surface.[2] And nucleolin on the cell surface tightly interacted with intracellular actin through an actin-based motor protein.[23] Large amounts of nucleolin on the cell surface probably reflect of the overexpression of nucleolin in cancer cells, and we found that the levels of nucleolin on the cell surface varied among five gastric cancer cell lines, although all levels were similarly overexpressed. The translocation of nucleolin in the gastric cancer cells is not well investigated, but we assume that tumor initiation is involved in some regulatory mechanism for localization of nucleolin.

Nucleolin on the cell surface reacted with only two antibodies, anti-NUC295 rabbit polyclonal antibody and a monoclonal antibody (mAbD3)[15,23]: it did not react with other commercially available antibodies, suggesting that nucleolin on the cell surface has a unique conformation with post-translational modification. *N*-Glycosylation of nucleolin is assumed to be essential for localization on the cell surface, based on our results showing that treatment of tunicamycin, an inhibitor of the *N*-linked glycosylation of protein, significantly reduced the amounts of nucleolin on the cell surface of MGT-40 cells, but not the amounts in nuclei.[3,24] Recently, *Vicia villosa* lectin (VVL)-positive nucleolin, which contains GalNAcα1-O-Ser/Thr glycosylation, was reported to be present in the cell membrane of melanoma cells.[21] Whether a similar glycosylation is found in nucleolin on the cell surface of gastric cancer cells needs to be investigated next.

Looking at the function of nucleolin on the cell surface, nucleolin acts as a receptor for various ligands. The binding complexes of nucleolin with ligands are internalized into the cells. HIV particle is one of its ligands, and the anti-HIV pseudopeptide HB-19, which specifically binds to nucleolin on the cell surface, prevents HIV infection.[11] Since HB-19 tightly binds to nucleolin and inhibits nucleolin function, HB-19 induces anticancer activity and inhibition of angiogenesis.[25] It is important to note that the DNA aptamer AS1411 binds to nucleolin on the cell surface, and rapidly internalizes into gastric cancer cells. We have presented the results showing that the growth inhibition of gastric cancer cells with AS1411 is associated with induction of S-phase arrest, and that AS1411 increases in sub-Go phase cells of MKN-45 cells and induces apoptosis. Also it is well understood that guanine-rich oligonucleotide induces S-phase arrest by inhibition of DNA synthesis.[26] Therefore, since neither AS1411 nor HB-19 show any toxic effects on normal cells, we think that the localization of nucleolin on the cell surface is a general feature of gastric cancer, and that a nucleolin targeted ligand would be a promising tool for gastric cancer treatment: AS1411 is now under Phase II clinical trials for acute myeloid leukemia and renal cancer in the United States.[12] In conclusion, nucleolin is an essential protein for cell proliferation, and the localization of nucleolin on the cell surface is unique in cancer cells. Moreover, study of the screening of nucleolin targeted ligands will intensify the understanding of carcinogenesis by *H. pylori* infection with Tipα.

Acknowledgments This work was supported by the Japan Society for the Promotion of Science, and by the Smoking Research Fund. We thank Drs. Kei Nakachi and Tomonori Hayashi at Radiation Effects Research Foundation, Hiroshima, for their fruitful discussion, and also thank to Ms. Kaori Suzuki and Ikuko Shiotani, Research Institute for Clinical Oncology, Saitama Cancer Center, for their technical assistance.

REFERENCES AND NOTES

1) Storck S., Shukla M., Dimitrov S., Bouvet P., *Subcell. Biochem.*, **41**, 125—144 (2007).
2) Ginisty H., Sicard H., Roger B., Bouvet P., *J. Cell Sci.*, **112**, 761—772 (1999).
3) Watanabe T., Tsuge H., Imagawa T., Kise D., Hirano K., Beppu M., Takahashi A., Yamaguchi K., Fujiki H., Suganuma M., *J. Cancer Res. Clin. Oncol.*, DOI 10.1007/s00432-009-033 (2010).
4) Suganuma M., Kurusu M., Suzuki K., Nishizono A., Murakami K., Fujioka T., Fujiki H., *J. Cancer Res. Clin. Oncol.*, **131**, 305—313 (2005).
5) Suganuma M., Yamaguchi K., Ono Y., Matsumoto H., Hayashi T., Ogawa T., Imai K., Kuzuhara T., Nishizono A., Fujiki H., *Int. J. Cancer*, **123**, 117—122 (2008).
6) Giuffre G., Caruso R. A., Barresi G., Tuccari G., *Virchows Arch.*, **433**, 261—266 (1998).
7) Derenzini M., Sirri V., Trere D., Ochs R. L., *Lab. Invest.*, **73**, 497—502 (1995).
8) Said E. A., Krust B., Nisole S., Svab J., Briand J. P., Hovanessian A. G., *J. Biol. Chem.*, **277**, 37492—37502 (2002).
9) Legrand D., Vigie K., Said E. A., Elass E., Masson M., Slomianny M. C., Carpentier M., Briand J. P., Mazurier J., Hovanessian A. G., *Eur. J.*

Biochem., **271**, 303—317 (2004).
10) Shi H., Huang Y., Zhou H., Song X., Yuan S., Fu Y., Luo Y., *Blood*, **110**, 2899—2906 (2007).
11) Nisole S., Said E. A., Mische C., Prevost M. C., Krust B., Bouvet P., Bianco A., Briand J. P., Hovanessian A. G., *J. Biol. Chem.*, **277**, 20877—20886 (2002).
12) Ireson C. R., Kelland L. R., *Mol. Cancer Ther.*, **5**, 2957—2962 (2006).
13) Soundararajan S., Chen W., Spicer E. K., Courtenay-Luck N., Fernandes D. J., *Cancer Res.*, **68**, 2358—2365 (2008).
14) Ichinose M., Nakanishi H., Fujino S., Tatematsu M., *Jpn. J. Cancer Res.*, **89**, 516—524 (1998).
15) Hirano K., Miki Y., Hirai Y., Sato R., Itoh T., Hayashi A., Yamanaka M., Eda S., Beppu M., *J. Biol. Chem.*, **280**, 39284—39293 (2005).
16) Komori A., Yatsunami J., Okabe S., Abe S., Hara K., Suganuma M., Kim S. J., Fujiki H., *Jpn. J. Clin. Oncol.*, **23**, 186—190 (1993).
17) Okabe S., Suganuma M., Hayashi M., Sueoka E., Komori A., Fujiki H., *Jpn. J. Cancer Res.*, **88**, 639—643 (1997).
18) Suganuma M., Okabe S., Marino M. W., Sakai A., Sueoka E., Fujiki H., *Cancer Res.*, **59**, 4516—4518 (1999).
19) Suganuma M., Okabe S., Kurusu M., Iida N., Ohshima S., Saeki Y., Kishimoto T., Fujiki H., *Int. J. Oncol.*, **20**, 131—136 (2002).
20) Semenkovich C. F., Ostlund R. E. Jr., Olson M. O., Yang J. W., *Biochemistry*, **29**, 9708—9713 (1990).
21) Hoja-Lukowicz D., Przybylo M., Pochec E., Drabik A., Silberring J., Kremser M., Schadendorf D., Laidler P., Litynska A., *Cancer Immunol. Immunother.*, **58**, 1471—1480 (2009).
22) Takaishi S., Okumura T., Tu S., Wang S. S., Shibata W., Vigneshwaran R., Gordon S. A., Shimada Y., Wang T. C., *Stem Cells*, **27**, 1006—1020 (2009).
23) Hovanessian A. G., Puvion-Dutilleul F., Nisole S., Svab J., Perret E., Deng J. S., Krust B., *Exp. Cell Res.*, **261**, 312—328 (2000).
24) Losfeld M. E., Khoury D. E., Mariot P., Carpentier M., Krust B., Briand J. P., Mazurier J., Hovanessian A. G., Legrand D., *Exp. Cell Res.*, **315**, 357—369 (2009).
25) Destouches D., El Khoury D., Hamma-Kourbali Y., Krust B., Albanese P., Katsoris P., Guichard G., Briand J. P., Courty J., Hovanessian A. G., *PLoS One*, **3**, e2518 (2008).
26) Xu X., Hamhouyia F., Thomas S. D., Burke T. J., Girvan A. C., McGregor W. G., Trent J. O., Miller D. M., Bates P. J., *J. Biol. Chem.*, **276**, 43221—43230 (2001).

J Cancer Res Clin Oncol (2010) 136
DOI 10.1007/s00432-009-0733-y

ORIGINAL PAPER

Nucleolin as cell surface receptor for tumor necrosis factor-α inducing protein: a carcinogenic factor of *Helicobacter pylori*

Tatsuro Watanabe · Hideaki Tsuge · Takahito Imagawa · Daisuke Kise · Kazuya Hirano · Masatoshi Beppu · Atsushi Takahashi · Kensei Yamaguchi · Hirota Fujiki · Masami Suganuma

Received: 22 October 2009 / Accepted: 13 November 2009 / Published online: 5 January 2010

Abstract
Purpose Tumor necrosis factor-α inducing protein (Tipα) is a unique carcinogenic factor released from *Helicobacter pylori* (*H. pylori*). Tipα specifically binds to cells and is incorporated into cytosol and nucleus, where it strongly induces expression of *TNF-α* and *chemokine* genes mediated through NF-κB activation, resulting in tumor development. To elucidate mechanism of action of Tipα, we studied a binding protein of Tipα in gastric epithelial cells.
Methods Tipα binding protein was found in cell lysates of mouse gastric cancer cell line MGT-40 by FLAG-pull down assay and identified to be cell surface nucleolin by flow cytometry using anti-nucleolin antibody. Incorporation of Tipα into the cells was determined by Western blotting and expression of *TNF-α* gene was quantified by RT-PCR.
Results Nucleolin was co-precipitated with Tipα-FLAG, but not with del-Tipα-FLAG (an inactive mutant). After treatment with Tipα-FLAG, incorporated Tipα was co-immunoprecipitated with endogenous nucleolin using anti-nucleolin antibody. The direct binding of Tipα to recombinant His-tagged nucleolin fragment (284–710) was also confirmed. Although nucleolin is an abundant non-ribosomal protein of the nucleolus, we found that nucleolin is present on the cell surface of MGT-40 cells. Pretreatment with anti-nucleolin antibody enhanced Tipα-incorporation into the cells through nucleolin internalization. In addition, pretreatment with tunicamycin, an inhibitor of N-glycosylation, decreased the amounts of cell surface nucleolin and inhibited both internalization of Tipα and expression of *TNF-α* gene.
Conclusions All the results indicate that nucleolin acts as a receptor for Tipα and shuttles Tipα from cell surface to cytosol and nuclei. These findings provide a new mechanistic insight into gastric cancer development with Tipα.

Keywords Gastric cancer · TNF-α · NF-κB · *Helicobacter pylori* · Tumor promotion

Abbreviations

H. pylori	*Helicobacter pylori*
Tipα	TNF-α inducing protein
CagA	Cytotoxin associated antigen
LC–MS	Liquid chromatography–mass spectrometry
RBD	RNA binding domain
NF-κB	Nuclear factor-kappa B
NEMO	NF-κB essential modulator

T. Watanabe · A. Takahashi · M. Suganuma (✉)
Saitama Cancer Center, Research Institute for Clinical Oncology, Kitaadachi-gun, Saitama 362-0806, Japan
e-mail: masami@cancer-c.pref.saitama.jp

T. Watanabe · A. Takahashi
Graduate School of Science and Engineering, Saitama University, Sakura-ku, Saitama 338-8570, Japan

H. Tsuge · T. Imagawa
Institute for Health Sciences, Tokushima Bunri University, Tokushima 770-8514, Japan

D. Kise · H. Fujiki
Faculty of Pharmaceutical Sciences, Tokushima Bunri University, Tokushima 770-8514, Japan

K. Hirano · M. Beppu
Tokyo University of Pharmacy and Life Science, Hachioji, Tokyo 192-0392, Japan

K. Yamaguchi
Hospital, Saitama Cancer Center, Saitama 362-0806, Japan

Introduction

Helicobacter pylori (*H. pylori*) is a gram-negative bacterium that colonizes in the mucosa of human stomach, resulting in induction of chronic gastritis, peptic ulcer, and stomach cancer (IARC Working Group on the Evaluation of Carcinogenic Risks to Humans 1994, Peek and Blaser 2002). Key criteria of these clinical outcomes are the severity and persistence of inflammation caused by *H. pylori*-infection, associated with strong induction of inflammatory cytokines, such as tumor necrosis factor-α (TNF-α), interleukine-1 (IL-1) and chemokines (El-Omar et al. 2000; Peek 2008; Snaith and El-Omar 2008). It is well accepted that inflammatory cytokines contribute to maintain cancer microenvironment (Balkwill 2009; El-Omar et al. 2003), and among the inflammatory cytokines, TNF-α plays a master role as an endogenous tumor promoter in carcinogenesis (Balkwill 2009; Moore et al. 1999; Suganuma et al. 1999). Moreover, TNF-α released from the cells acts as an instigator of a cytokine network sequence, from TNF-α to IL-1 and IL-6 and back to TNF-α, maintaining inflammation in the process of tumor promotion (Suganuma et al. 2002).

To extend the concept, a new gene, *TNF-α inducing protein* (*Tipα*) gene, was cloned from the genome of *H. pylori* strain 26695. Tipα directly induces *TNF-α* gene expression in gastric epithelial cells (Suganuma et al. 2005, 2006, 2008). The unique features of Tipα protein are as follows: (1) *H. pylori* lacking *Tipα* gene reduced the colonization levels of *H. pylori* in the stomach of mice (Godlewska et al. 2008); (2) Vaccination with Tipα significantly reduced colonization of *H. pylori* in mice associated with high levels of Tipα-specific antibody (Inoue et al. 2009); (3) Tipα protein is secreted from *H. pylori* but not mediated through Type IV secretion system (Suganuma et al. 2005); and (4) clinical isolates of *H. pylori* obtained from gastric cancer patients secreted Tipα protein in larger amounts than did *H. pylori* from patients with simple gastritis (Suganuma et al. 2008), strongly suggesting that Tipα plays an important role in *H. pylori*-induced inflammation and cancer development in human stomach (Balkwill 2009). All these features are different from those of other virulence factors, such as the cag pathogenicity island (cagPAI), CagA (cytotoxin associated antigen) and VacA (vacuolating cytotoxin A).

Members of the *Tipα* gene family include *Tipα* itself, *H. pylori-membrane protein 1* (*HP-MP1*), and *jph0543*, and these do not have any obvious homologues in other species (Suganuma et al. 2005; Yoshida et al. 1999). Tipα protein consists of 172 amino acids with a molecular weight of 19 kDa, and it forms a homodimer via two disulfide bonds with two cysteine residues in the N-terminal region. We previously reported that homodimer formation of Tipα is essential for induction of *TNF-α* gene expression in gastric epithelial cells (Suganuma et al. 2008) and also for transformation of Bhas 42 (v-H-*ras* transfected BALB/3T3) cells (Suganuma et al. 2005). To extend our experiments, we made two inactive Tipα mutants: a deletion mutant of Tipα (del-Tipα) that deleted six amino acids including two cysteine residues from native Tipα, and C5A/C7A double mutant (C5A/C7A-Tipα), two cysteine residues of Tipα are replaced by two alanines. The two mutated Tipα proteins induced *TNF-α* gene expression less strongly than native Tipα did (Suganuma et al. 2008). The crystal structures of del-Tipα and truncated forms of Tipα were recently reported by three independent groups, which revealed that they take dimerized forms, although they do not have the full length of protein (Jang et al. 2009; Tosi et al. 2009; Tsuge et al. 2009). If so, it is understandable that del-Tipα has weak activity.

We also found that fluorescence-labeled Tipα specifically binds to the surface of MGT-40 cells and enters into the cytosol and nuclei, whereas del-Tipα and C5A/C7A-Tipα bind weakly to the cells (Suganuma et al. 2008). In the light of this evidence, we think that homodimers of Tipα can easily bind to a specific receptor molecule on the cell surface of gastric epithelial cells. We identified nucleolin as a specific receptor of Tipα on the cell surface using pull-down assay with anti-FLAG antibody against FLAG-tagged Tipα protein. Nucleolin is a well-known major non-ribosomal protein consisting of 710 amino acids in nucleolus, and it has three different structural domains: an N-terminal domain containing highly acidic residues, a central domain containing four RNA recognition motifs, and a C-terminal domain containing Arg-Gly-Gly (RGG) repeats (Ginisty et al. 1999). Nucleolin is known to have multi-functions, including chromatin remodeling, DNA recombination, DNA replication, RNA transcription by RNA polymerase I and II, rRNA processing, mRNA stabilization, cytokinesis and apoptosis (Ginisty et al. 1999; Storck et al. 2007). Furthermore, recent evidence indicates that nucleolin is present on the surface of a wide range of cancer cells and some other types of the cells, and acts as receptors for several molecules (Hirano et al. 2005; Hoja-Lukowicz et al. 2009; Hovanessian et al. 2000; Legrand et al. 2004; Reyes-Reyes and Akiyama 2008). To investigate the specific interaction of nucleolin with Tipα, we conducted experiments to characterize localization of nucleolin, and studied the internalization of Tipα and subsequent induction of *TNF-α* gene expression. This paper reports for the first time that nucleolin is clearly involved in the carcinogenic process of *H. pylori* as a major cellular receptor of Tipα protein.

Materials and methods

Cell culture and reagents

Mouse gastric cancer cell line MGT-40 was maintained in DMEM with 10% fetal bovine serum (JRH Bioscience) and MITO+ serum extender (Becton–Dickinson Labware), as described previously (Ichinose et al. 1998). Human gastric cancer cell line MKN-1 and human monocytic leukemia cell line THP-1 were grown in RPMI 1640 medium with 10% fetal bovine serum. Anti-Tipα antibody was raised in rabbits by immunizing a synthetic peptide of 19 amino acids (from 11 to 29) of Tipα, and anti-nucleolin antibody (anti-NUC295) was raised in rabbits by immunizing a syntheic peptide of eight amino acids (from 295 to 302) of nucleolin, as described previously (Hirano et al. 2005; Suganuma et al. 2005). Other anti-nucleolin antibodies were purchased from Santa Cruz Biotethnology and Bethyl Laboratories, Inc. Anti-HSP90, anti-epidermal growth factor (EGF) receptor, anti-TNF receptor 2 and anti-lamin B antibodies were purchased from Santa Cruz Biotethnology. Anti-FLAG antibody was obtained from Sigma.

Preparation of three different *Tipα* genes tagged with FLAG

Three genes encoding Tipα-FLAG, del-Tipα-FLAG and C5A/C7A-Tipα-FLAG were obtained by PCR of pET28(a)$^+$-Tipα (Suganuma et al. 2005) containing oligonucleotide primers: Tipα-FLAG_F (5′-AGAGCATATGCT GCAGGCTTGCACTTGCCC) and Tipα-FLAG_R (5′-GG ATCCTACTTATCGTCGTCATCCTTGGTAGTCCATG GCTATAGG), del-Tipα-FLAG_F (5′-AGAGCATATGC CAAACACTTCACAAAGGAA), del-Tipα-FLAG_R (5′-G GATCCTACTTATCGTCGTCATCCTTGGTAGTCCAT GGCTATAGG), and C5A/C7A-Tipα-FLAG_F (5′-CA GCCATATGCTGCAGGCTGCCACTGCCCCAAACA C), C5A/C7A-Tipα-FLAG_R (5′-GGATCCTACTTATCG TCGTCATCCTTGGTAGTCCATGGCTATAGG). Three amplified fragments were separately cloned into a pET28(a)$^+$ expression vector (Invitrogen).

Preparation of three FLAG-tagged Tipα proteins

Each FLAG-tagged protein was expressed in *E. coli* (DE3) transfected pET28(a)$^+$ expression vector containing each of the corresponding genes above mentioned. They were induced with isopropyl-β-D-thiogalactopyranoside, and then purified by Ni^{2+} chelating resin (Ni Sepharose 6 Fast Flow, GE Healthcare), as reported previously (Suganuma et al. 2005). Tipα-FLAG, del-Tipα-FLAG and C5A/C7A-Tipα-FLAG all carry a tag of six histidines at the N-terminal region and also a FLAG-tag at the C-terminal region (Fig. 1a). All three recombinant Tipα proteins were more than 98% pure on SDS-PAGE. To conduct Ni^{2+} affinity pull-down assay, His-tag-removed Tipα-FLAG and His-tag-removed C5A/C7A-Tipα-FLAG proteins were prepared as follows: His-tagged Tipα-FLAG and C5A/C7A-Tipα-FLAG proteins were cleaved at a thrombin cleavage cite

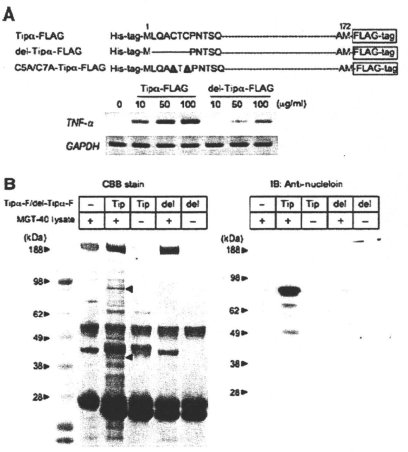

Fig. 1 Identification of nucleolin as Tipα binding protein. **a** Schematic representation of Tipα-FLAG, del-Tipα-FLAG and C5A/C7A-Tipα-FLAG proteins (*top*). Induction of *TNF-α* gene expression with Tipα-FLAG and with del-Tipα-FLAG in MGT-40 cells (*bottom*). Total RNAs were isolated from MGT-40 cells 1 h after treatment with Tipα-FLAG and with del-Tipα-FLAG, and the levels of TNF-α and GAPDH mRNAs were determined by semi-quantitative RT-PCR, as described in Materials and methods. **b** Representative results of FLAG pull-down assay. After incubation of MGT-40 cell lysates with Tipα-FLAG (Tip) and with del-Tipα-FLAG (del), Tipα-FLAG and del-Tipα-FLAG were immunoprecipitated with anti-FLAG antibody. The polypeptides that co-immunoprecipitated with Tipα-FLAG and with del-Tipα-FLAG were resolved in 4–12% NuPAGE and then stained with Quick CBB (*left panel*) and immunoblotted with anti-nucleolin antibody (IB: *right panel*). **c** Amino acid sequence of mouse nucleolin. Amino acids with *red characters* are assigned to the sequences determined by LC–MS analysis. *Underlined sequences* are recognition sites of anti-NUC295

using Thrombin cleavage capture kit (Novagen). Then the cleaved His-tag-peptide and uncleaved protein were separated using Ni^{2+} chelating resin (Tsuge et al. 2009).

Preparation of His-tagged nucleolin protein fragment

His-tagged nucleolin gene fragment (*NUC284*), containing both residues from 284 to 710 of human nucleolin and C-terminal His-tag, was expressed in *E. coli* transfected pBAD/Thio-E/NUC284 expression vector, and purified by Ni^{2+} chelating resin, as described previously (Hirano et al. 2005).

Expression of *TNF*-α gene

MGT-40 and THP-1 cells were treated with recombinant protein for 1 h, and total RNAs obtained from the cells were isolated with ISOGEN reagent (Nippon Gene). Expressions of *TNF*-α gene and *glyceraldehyde-3-phosphate dehydrogenase* (*GAPDH*) gene as a control were determined by both semi-quantitative RT-PCR and real-time RT-PCR, as described previously (Suganuma et al. 2005). The values are expressed as the average of three separate experiments.

FLAG pull-down assay

MGT-40 cell lysates were prepared with NP-40 lysis buffer containing 20 mM Tris–HCl (pH 7.4), 100 mM NaCl, 0.5% NP-40, 10% glycerol, 1 mM PMSF, 1 μg/ml aprotinin, and 1 μg/ml leupeptin, and the lysates (600 μg/ml) were incubated with Tipα-FLAG (200 μg/ml) and del-Tipα-FLAG (200 μg/ml) in buffer A containing 50 mM Tris–HCl (pH 7.4), 150 mM NaCl, 1 mM PMSF, 1 μg/ml aprotinin, and 1 μg/ml leupeptin at 4°C for 2 h. After addition of 20 μl anti-FLAG M2 Gel (Sigma), the mixture was further incubated at 4°C for 2 h, and then the resin was washed with buffer A containing 1% Triton X-100. The polypeptides associated with the resin were resolved in 4–12% NuPAGE (Invitrogen), and were determined using staining with Quick CBB (Wako). The control experiments were similarly conducted without using Tipα-FLAG and del-Tipα-FLAG.

LC–MS analysis

Gel sections containing polypeptides co-precipitated with Tipα-FLAG were subjected to proteolysis with 2 μg/ml trypsin (Wako) at 25°C overnight, and the digestion was stopped by adding an elution solution (50% acetonitrile, 5% formic acid). Each sample was analyzed using Nano-ESI-Ion trap MS (HCT plus, Bruker Daltonics), according to manufacturer's instruction (Bruker application note). The data were analyzed by a protein database search on MASCOT (Matrix Science).

Ni^{2+} affinity pull-down assay

His-tagged nucleolin fragment (NUC284) was incubated with His-tag-removed Tipα-FLAG or His-tag-removed C5A/C7A-Tipα-FLAG in NP-40 lysis buffer containing 10 mM imidazole at 4°C for 2 h. Twenty microlitre of Ni^{2+} chelating resin was then added to the mixture, which was further incubated at 4°C for 2 h. After washing the resin with NP-40 lysis buffer containing 40 mM imidazole, the complex of nucleolin fragment (NUC284) with Tipα-FLAG or with C5A/C7A-Tipα-FLAG were determined by Western blotting using anti-nucleolin (H-250, Santa Cruz) and anti-Tipα antibodies, respectively.

Incorporation of Tipα into cells

MGT-40 cells were treated with Tipα, and then lysed in lysis buffer containing 20 mM Tris–HCl (pH 8.0), 150 mM NaCl, 1% Triton X-100, 0.1% SDS, 1% sodium deoxycholate, 1 mM PMSF, 1 μg/ml aprotinin, and 1 μg/ml leupeptin. Cell lysates were resolved in 12% SDS-PAGE. Incorporation of Tipα into the cells was determined by Western blotting using anti-Tipα antibody (Suganuma et al. 2008).

Analysis of subcellular fractionation

Homogenates of MGT-40 and THP-1 cells were fractionated into membrane, cytosol, and nuclei using Qproteome cell compartment kit (Qiagen), according to the manufacturer's instruction. Each fraction was subjected to Western blotting, using anti-nucleolin, anti-HSP90 (a marker for cytosol), anti-EGFR or anti-TNF receptor 2 (for membrane) and anti-lamin B antibodies (for nuclei).

Immunoprecipitation

MKN-1 and THP-1 cells were treated with Tipα-FLAG and del-Tipα-FLAG at a concentration of 100 μg/ml at 37°C for 1 h, and then lysed as described above. Cell lysates (about 400 μg) were incubated with anti-nucleolin antibody (A300-711A, Bethyl Lab, Inc.) at 4°C for 2 h. The immunocomplex was captured with protein A sepharose (GE Healthcare) at 4°C overnight, and then washed with NP-40 lysis buffer. The immunocomplex was applied to 12% SDS-PAGE. Tipα-FLAG, del-Tipα-FLAG and nucleolin were determined by Western blotting using anti-FLAG and anti-nucleolin antibodies (MS-3, Santa Cruz).

Flow cytometry

MGT-40 and THP-1 cells (1×10^6 cells/ml) in PBS were incubated with 2 μg/ml anti-NUC295 antibody and 10 μg/ml Alexa Fluor 488-conjugated goat anti-rabbit IgG (Invitrogen) on ice for 30 min. Then cells were subjected to flow cytometry (Epics XL, Beckman Coulter).

Statistical analysis

The data were compared using Student's *t* test.

Results

Identification of nucleolin as a Tipα-binding protein

To characterize the nature of the specific binding protein for Tipα, Tipα tagged with FLAG at C-terminus (Tipα-FLAG) and del-Tipα tagged with FLAG at C-terminus (del-Tipα-FLAG)—the latter with six amino acids deleted including two cysteine residues from N-terminal region of Tipα—were used for the experiments (Fig. 1a). Tipα-FLAG protein induced *TNF-α* gene expression in mouse gastric cancer cells (MGT-40), while del-Tipα-FLAG was over ten times weaker than Tipα-FLAG. Thus, Tipα-FLAG and del-Tipα-FLAG showed the same biological activity as did recombinant Tipα and del-Tipα (Fig. 1a).

The mixtures of MGT-40 cell lysates with Tipα-FLAG and with del-Tipα-FLAG were separately subjected to pull-down assay using resin conjugated with anti-FLAG antibody. Thirteen polypeptide bands on SDS-PAGE were found to be co-precipitated with Tipα-FLAG, but not with del-Tipα-FLAG (Fig. 1b). Each polypeptide band was subjected to LC–MS analysis after tryptic digestion, and it turned out that the amino acid sequences of two polypeptides, with 88 and 40 kDa, were similar to that of mouse nucleolin, as shown in Fig. 1c. The results showed that the polypeptide with 88 kDa is nucleolin and the other polypeptide with 40 kDa is a fragment of nucleolin. Three polypeptides with less than 40 kDa were derived from Tipα, and another polypeptide with less than 50 kDa was identical to ribosomal protein L4 fragment; the others could not be confirmed by LC–MS.

The polypeptide with 88 kDa was further confirmed to be nucleolin using immunoblot analysis with anti-nucleolin antibody, but the polypeptide with 40 kDa did not react with anti-nucleolin antibody (Fig. 1b), probably because the latter peptide did not contain recognition sites of the antibody. Although several polypeptides with 50–70 kDa reacted with anti-nucleolin antibody, we think that there were degradation fragments of nucleolin co-precipitated with Tipα-FLAG. The results strongly suggest that nucleolin acts as a specific binding protein of Tipα.

Interaction of incorporated Tipα with endogenous nucleolin in the cells

The binding of Tipα to nucleolin at cellular levels was examined by immunoprecipitation using anti-nucleolin antibody. Since the affinity of the anti-nucleolin antibody for human nucleolin is higher than that for mouse nucleolin, we used cell lysates of both human gastric cancer cell lines MKN-1 and human monocytic leukemia cell line THP-1 for the experiments. Significant amounts of Tipα-FLAG interacted with the lysates of MKN-1 and THP-1 cells, but the amounts of del-Tipα-FLAG interacted less with their cell lysates, which shows that both Tipα-FLAG and del-Tipα-FLAG were incorporated into the cells (Fig. 2a). Using anti-nucleolin antibody, these cell lysates were further subjected to immunoprecipitation: nucleolin was immunoprecipitated with anti-nucleolin antibody associated with Tipα-FLAG but not del-Tipα-FALG in both MKN-1 and THP-1 cells (Fig. 2a). These results suggest that Tipα directly binds to native and endogenous nucleolin in the cells, and the differences of binding ability between Tipα-FLAG and del-Tipα-FLAG to nucleolin are comparable to their inducing potencies of *TNF-α* gene expression.

Direct interaction of nucleolin with Tipα

Next, we studied whether Tipα directly binds to recombinant human nucleolin fragment NUC284, which consists of amino acids from 284 to 710 containing four RNA binding domains. His-tag-removed Tipα-FLAG was incubated in vitro with NUC284 fragment and Ni^{2+} chelating resin, and we found that Tipα-FLAG significantly co-precipitated with NUC284 fragment, although small amounts of Tipα-FLAG precipitated with Ni^{2+} chelating resin only (Fig. 2b). However, His-tag-removed C5A/C7A-Tipα-FLAG did not co-precipitate with NUC284 fragment, suggesting that the homodimer form of Tipα is necessary for direct binding to nucleolin: We think that the homodimer of Tipα directly binds to two-thirds of C-terminal nucleolin, without any scaffold proteins.

Cell surface localization of nucleolin on MGT-40 cells

We previously reported that FITC-labeled Tipα specifically binds to the cell surface of MGT-40 cells (Suganuma et al. 2008). Since nucleolin is present on both nucleolus and surface of the cells (Barel et al. 2008; Hirano et al. 2005; Hoja-Lukowicz et al. 2009: Hovanessian et al. 2000; Legrand et al. 2004; Reyes-Reyes and Akiyama 2008),